On the average, numerical results have shown that the computing speed for the closed-form solution is approximately 25 times faster than the computing speed for the integration procedure. Needless to say, if more perturbations are added to the analysis, the rise and set times will be computed to greater accuracy at little expense in machine time.

References

[1] Baker, R. M. L., Jr. and Makemson, M. W., *An Introduction to Astrodynamics* (Academic Press, New York, 1960), pp. 313–320.

[2] Herrick, S., *Astrodynamics* (D. Van Nostrand, New York, in press), Chap. 6.

OCTOBER 1963 AIAA JOURNAL VOL. 1, NO. 10

Self-Contained Satellite Navigation Systems

M. Frazier,* B. Kriegsman,† and F. William Nesline Jr.‡
Raytheon Company, Bedford, Mass.

Two self-contained navigation systems are described for use in a satellite travelling around a planet in an elliptical orbit. The navigation sensor for both systems is a horizon scanner that provides two pieces of data: the local vertical and the width of the planet disk. The difference between the navigation systems is the method of processing the data. One method of data processing approximates the local vertical and the disk width by polynomials in time. Using a linear filter, the polynomial fitting the data with minimum squared error is generated. Certain coefficients of this polynomial are the desired position and velocity. In the second method of data processing, the orbital parameters that fit the measurement data with minimum squared error are generated. Position and velocity are derived from these orbital parameters. Navigational accuracy is determined for both systems. Numerical results are presented to show the effect on accuracy of variations in eccentricity, major axis, accuracy of measurement data, location of satellite in orbit, and noise bandwidth. It is shown that exact fitting reduces position errors by as much as a factor of 3 and velocity errors by as much as a factor of 10 compared to polynomial fitting.

Instrumentation

BOTH orbital-rendezvous and lunar-landing missions require accurate navigation of vehicles in elliptical orbits over time intervals of 20 hr or more. For reasons of simplicity and reliability it is desirable that the navigation system be self-contained. The navigation system of interest here accomplishes this by making use of a horizon scanner in combination with a stellar-monitored inertial reference platform. The horizon scanner provides the basic measurements of the orientation of the local vertical and the width of the planet disk. The navigation quantities of interest (vehicle position and velocity) are obtained by processing and smoothing these data in an appropriate manner. The azimuth orientation of the orbital plane with respect to the planet enclosed by the orbit is determined by taking fixes on at least two stars. The subject of this paper is the method of processing the horizon-scanner data.

The desired accuracy for the navigation information in the applications under consideration is 0.5 naut miles in position and 1 fps in velocity. The factors involved in the establishment of these requirements are described in Ref. 1 for an orbital-rendezvous mission. The major consideration here is that the ferry be transferred from parking orbit to a point sufficiently close to the satellite so that its radar seeker will be able to lock on to the satellite. For the case of a soft landing on the moon, it is important that the touchdown velocity be accurately controlled both in magnitude and direction in order to prevent tumbling and damage to the landing vehicle. For a representative three-legged landing vehicle, it is desirable that the vertical component of landing velocity be at least twice as large as the horizontal component to insure satisfactory stability.[2] If an inertial guidance system is used for determination of landing velocity, then it is important that the vehicle's velocity be accurately determined in the lunar parking orbit, prior to the final descent.

The most reliable method for sensing the horizon discontinuity of a planet such as the earth or moon is by measurement of the sharp gradient of infrared radiation between the edge of the body and outer space.[3] For the best performance it is desirable that the horizon sensor respond only to emitted thermal radiation from the planet, ignoring the reflected solar radiation.[4]

There are many different methods that have been developed and proposed for determining the horizon discontinuity of a planet.[3–8] One type of scanning system, which has been successfully used in experimental Atlas and Thor nose cones, test flown in a Jupiter missile, and is being used in the Project Mercury space capsule is shown in Fig. 1. The field of view of the detector (2° × 8°) is deflected by a scanning prism at an angle of 55° from the normal. A drive motor rotates the scanning prism at 30 rps, forming a 110° conical scan pattern as shown in Fig. 1. The difference in radiance level between the planet and outer space detected by the sensor causes a 30 cps rectangular wave to be generated. By comparing the phase of this rectangular wave with an internally generated reference signal, it is possible to determine the orientation of the pitch or roll axis of the vehicle with respect to the local vertical. A pair of these horizon sensors, oriented at right angles to each other as in Fig. 1, determine the orientation of the vehicle relative to the vertical.

Presented at the ARS 17th Annual Meeting and Space Flight Exposition, Los Angeles, Calif., November 13–18, 1962; revision received July 17, 1963.

* Senior Research Engineer, Space and Information Systems Division. Member AIAA.

† Principal Engineer, Missile Systems Division. Member AIAA.

‡ Manager, Analytical Research Department, Space and Information Systems Divsion. Member AIAA.

An alternate method of horizon sensing[4, 6] employs four horizon sensors oriented 90° apart from each other, as shown in Fig. 2. Each sensor employs a 0.5° × 3° field of view detector whose image is oscillated radially about the horizon discontinuity point over an angle of 4.5°. A servo-driven positioning mirror centers each of the scans on the discontinuity point to an accuracy of 0.1°. Each opposing pair of sensors (180° apart from each other) provides local-vertical orientation and planet disk width information. This type of horizon-scanning system is inherently more accurate, is capable of operation at higher altitudes, and possesses a longer lifetime potential than the conical-scanning system.[4]

Sources of Error in Horizon-Scanning System

There are several different sources of errors in the measurement of local vertical and planet disk width by means of a horizon scanner in combination with a stellar-monitored reference platform. Some of the more important of these error sources are the following: 1) horizon-scanner instrumentation errors, i.e., uncertainties in centering the sensor scan on the horizon discontinuity point because of factors such as detector noise, mechanical tolerances in the scanner, and mounting vibrations of scanner; 2) oblateness or ellipticity of the planet; 3) anomalies or irregularities of the surface of the planet; 4) uncertainties in the horizon discontinuity point because of atmospheric effects; 5) presence of clouds around the planet; and 6) uncertainties in the stellar-monitored reference platform.

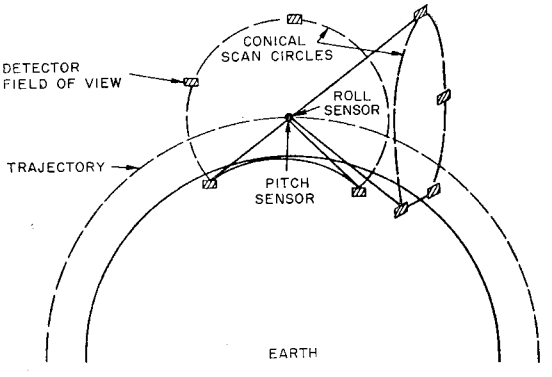

Fig. 1 Two-sensor conical scan IR horizon scanner.

Certain errors such as the deviation of the planet's shape from a sphere, i.e., oblateness effects, can be predicted fairly accurately as a function of the location of the vehicle with respect to the planet. Other errors such as unpredictable bias errors in the horizon-scanner instrument or in the stellar-monitored reference platform will remain essentially invariant over the time intervals of interest. Data smoothing or filtering techniques will not reduce the effects of these bias errors. Certain error sources such as the presence of clouds, atmospheric effects, and instrumentation imperfections will contribute both random time-varying errors and time-invariant bias errors. Under these conditions, it will be possible to correct for the bias errors only to the extent that they are predictable. It will, on the other hand, be possible to reduce greatly the effects of the random errors by appropriate data smoothing and processing techniques. The purpose of this paper is to show the reduction of random errors in horizon-scanner measurements that can be accomplished by the use of smoothing techniques.

Polynomial Smoothing

Data Processing

This section shows how to apply the polynomial smoothing concept to generate navigational information from local vertical and disk width measurements. It is shown that the polynomial that best fits the measurement, in a least squares sense, can be generated by passing these measurements through a linear, finite memory filter. Finally, the technique for deriving position and velocity information from this polynomial is presented.

Let $\theta_M(t_1 - \tau)$ and $r_M(t_1 - \tau)$ be the values of the local vertical θ and the radius r at time $t_1 - \tau$, which are calculated directly from the measured disk width and local vertical angular data. Then the least-squares fitting problem requires the minimization of the quantities E and F over the smoothing interval T, where E and F are given by the relation

$$E = \frac{1}{T}\int_0^T [\theta(\tau) - \theta_M(t_1 - \tau)]^2\, d\tau \tag{1}$$

$$F = \frac{1}{T}\int_0^T [r(\tau) - r_M(t_1 - \tau)]^2\, d\tau \tag{2}$$

To simplify the discussion, only the problem of least-squares fitting θ to θ_M will be considered. The procedure for fitting r to r_M is essentially identical to that for fitting θ to θ_M.

If Eq. (1) is now rewritten in the form

$$E = \frac{1}{T}\int_0^T [C_0 + C_1\tau + C_2\tau^2 + C_3\tau^3 + \ldots - \theta_M(t_1 - \tau)]^2\, d\tau \tag{3}$$

the partial derivatives of E with respect to each of the constants C_n (i.e., $\partial E/\partial C_n$) will, when set equal to zero, yield a set of linear algebraic equations in terms of the n unknown coefficients C_n.

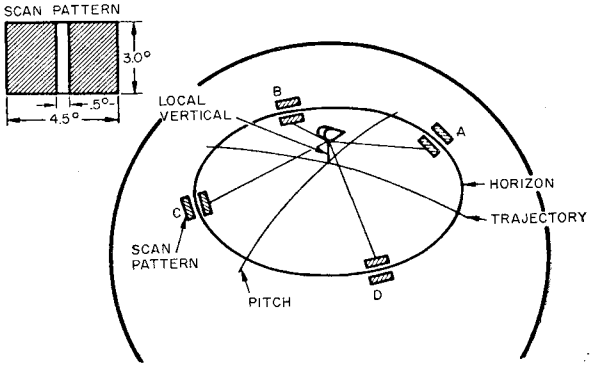

Fig. 2 Four-sensor linear scan IR horizon scanner.

The solution for any desired C_i is merely a linear combination of independent variables, e.g.,

$$C_i = \int_0^T (b_0 + b_1\tau + b_2\tau^2 + \ldots + b_n\tau^n)\theta_M(t_1 - \tau)d\tau \tag{4}$$

where the b_i terms are known functions of the smoothing interval T. To those familiar with linear filter theory, it is immediately apparent from Eq. (4) that the coefficients C_i can be generated as the output of a linear filter whose input is $\theta_M(t_1)$. If the input of a linear filter having a unit impulse response or weighting function $W(t)$ is $e_i(t)$, then the output is given by the superposition integral:

$$e_0(t) = \int_0^\infty W(\tau)e_i(t - \tau)d\tau \tag{5}$$

Comparison of Eqs. (4) and (5) shows that

$$e_i(t - \tau) \langle\!= \theta_M(t_1 - \tau)$$

$$W(\tau) \langle\!= \begin{cases} b_0 + b_1\tau + b_2\tau^2 + \ldots + b_n\tau^n & \text{over interval 0 to } T \\ 0 & \text{outside of interval 0 to } T \end{cases} \tag{6}$$

$$e_0(t) \langle\!= C_i$$

Table 1 Effect of variations in order of filter on the navigation-system performance accuracies

Root-sum-squares, error in	Order of polynomial filter 2	3	4
θ, mrad	0.264	0.246	0.238
$\dot{\theta}$, mrad/sec	2.71×10^{-3}	2.13×10^{-13}	2.42×10^{-3}
X, ft	5630	5240	5080
$\dot{X}$, fps	57.6	45.4	51.7
r, ft	1560	1480	1415
$\dot{r}$, fps	20.6	14.9	16.3

Thus, for a given order filter and a given smoothing time, weighting functions can be calculated for every C_i. Since these weighting functions determine the complete polynomial, any function of the polynomial can also be calculated. In the problem of navigation being considered, only $\theta(0)$ and $\dot{\theta}(0)$ are required. In terms of the polynomial coefficients, these quantities are

$$\theta(0) = C_0$$

$$\dot{\theta}(0) = \left.\frac{d\theta}{dt}\right|_{t=t_1} = -\left.\frac{d\theta}{d\tau}\right|_{\tau=0} = -C_1 \tag{7}$$

Thus, local vertical and rate of change of local vertical are outputs of a linear, finite memory filter. In a similar manner, values of the coefficients K_i of the polynomial $r(\tau)$ can be determined, and from them the altitude and rate of change of altitude can be determined.

An important question still unanswered at this point is the method for determining the proper order of polynomials to which the measurement data should be fitted. Also important is the determination of the best smoothing interval T (back from present time t_1) over which the data should be filtered to minimize filter output errors. The following section of this paper will show the factors involved in the selection of the order of the polynomial fit and the smoothing interval T.

Error Analysis of Polynomial Smoothing Technique

There are two major sources of error in the output polynomial coefficients derived by passing the input signal through the linear polynomial filters: 1) random (white noise) fluctuations in the input signal to the filter; and 2) truncation errors arising because the polynomial used to fit the data is of finite order over the interval of interest, whereas the actual polynomial continues to arbitrarily high order.

An analysis of the random and truncation errors in the output polynomial coefficients derived by passing an input signal through the polynomial filters is given in Ref. 9. Important results from this analysis can be summarized as follows:

1) Random errors tend to increase as the order of the polynomial fit is increased; truncation errors, on the other hand, will decrease under these conditions.

2) Random errors tend to decrease as the smoothing interval T is increased; truncation errors, on the other hand, will increase under these conditions.

Thus, for a given order of polynomial fit there will be an optimum smoothing interval T_{opt} for which the root-sum-squares of the random and truncation errors in the filter output are a minimum. Likewise, there will be a certain order of fit for a given input signal, which will minimize the root-sum-squared output error (assuming that the proper T_{opt} is used for each order of fit). The magnitude of the output random error will vary as a function of the magnitude and bandwidth of the noise on the input signal. The magnitude of the truncation error depends upon the accuracy to which the selected polynomial represents the noise-free input signal over the smoothing interval of interest.

It should be noted carefully that the selection of the proper order of the polynomial filter and the optimum smoothing intervals are predicted on a priori knowledge of the characteristics of the input data θ_i.

The distance from the center of the earth to the vehicle (r) is obtained from horizon scanner measurements of the width of the earth disk by the following equation:

$$r = R/\sin\phi \tag{8}$$

where R is the radius of the earth, and ϕ is one-half of the angle subtended by the earth from the vehicle location. Since the basic measurement data going into the filter will be data of ϕ, whereas the desired outputs are r and $\dot{r}$, it is necessary to relate errors in ϕ to errors in r. By differentiating Eq. (8), the following relation is obtained between an error δr and an error $\delta\phi$:

$$\delta r = -\left[\frac{R\cos\phi}{\sin^2\phi}\right]\delta\phi \tag{9}$$

The coefficient $R\cos\phi/\sin^2\phi$ will not be exactly constant over the smoothing intervals of interest here because of variations in ϕ. For purposes of estimating errors, however, satisfactory accuracy can be obtained by using an average value of the coefficient $R\cos\phi/\sin^2\phi$ for the interval of interest.

The following data indicate the accuracy of navigation information attainable by the techniques of polynomial smoothing. Results are presented for both earth and lunar orbits. The effects on accuracy shown are of variations in orbit eccentricity ϵ, semimajor axis of orbit a, location of vehicle in orbit, the magnitude θ, and bandwidth F_0 of the measurement data. Numerical comparisons are also made between second-, third-, and fourth-order fits.

Before commencing the discussion and presentation of the numerical results, it is appropriate to list the nominal or reference values of the various system parameters. Unless explicitly stated to the contrary, it is assumed that the system parameters have the values given below:

Orbit eccentricity $\epsilon = 0.0275$
Present vehicle location = 45° past perigee
Orbit semimajor axis $a = 3640$ naut miles
Mean orbital angular velocity $\omega = 1.14 \times 10^{-3}$ rad/sec (earth orbit)
Magnitude of noise on input measurements (σ_θ and σ_ϕ) = 2 mrad
Bandwidth of Input Noise = 0.5 cps

The effect of variations in the order of the polynomial smoothing filter are summarized in Table 1. It should be noted that the data of Table 1 are based on the assumption of optimum smoothing-time intervals for filtering the various data. The values of the optimum smoothing intervals used in the data of Table 1 are shown in Table 2. The quantities X and $\dot{X}$ in these tables represent the horizontal position and velocity of the satellite, respectively.

From Table 1 it can be seen that the accuracy of the position and velocity information X, $\dot{X}$, r, and $\dot{r}$ is relatively insensitive to the order of the polynomial filter, for the assumed conditions. The highest accuracy in velocity information ($\dot{X}$ and $\dot{r}$) is found to be obtained by use of a third-order filter. The optimum smoothing intervals, as can be seen in

Table 2 Effect of variations in order of filter on the optimum-smoothing intervals for the measurement data

Optimum smoothing time for minimum root-sum-squares, error in	Order of polynomial filter 2	3	4
θ and X, sec	600	1180	2160
$\dot{\theta}$ and $\dot{X}$, sec	568	1145	2130
r, sec	488	900	1740
$\dot{r}$, sec	463	874	1720

Table 3 Effect of variations in nominal system parameters upon guidance system accuracies around the earth

Minimum root-sum-squares, error in	Nominal conditions	Orbit eccentricity, $\epsilon = 0.00275$	Location 90° after perigee	σ_θ, σ_ϕ, 5 mrad	σ_θ, σ_ϕ, 0.5 mrad	F_0, 0.05 cps	a, 4900 naut miles
X, ft	5240	4060	5440	11800	1530	14600	5810
X, fps	45.4	21.1	51.1	86.1	16.0	98.1	34.0
r, ft	1480	1150	1540	3320	432	4120	3200
$\dot{r}$, fps	14.9	6.92	16.8	28.6	5.28	32.2	18.8

Table 2, are fairly sensitive to the order of the filter. As the order of the filter increases, the smoothing interval is also increased.

The effect of variations in the nominal system parameters upon the guidance system accuracies are summarized in Table 3. The system performance, as can be seen, is improved by decreasing the orbit eccentricity ϵ and the magnitude of the noise on the input measurements σ_θ and σ_ϕ. It is particularly sensitive to variations in σ_θ and σ_ϕ. The system performance is relatively insensitive to the location of the vehicle in orbit and the magnitude of the semimajor axis of the orbit a.

The performance of the navigation system for earth and lunar orbits is compared in Table 4. The semimajor axis a for the earth orbit is taken as 3640 naut miles and for the lunar orbit as 1037 naut miles. The values of the other important system parameters, ϵ, F_0, σ_θ, and σ_ϕ, are taken as the same for the nominal conditions. Third-order polynomial filters are used here with optimum values of the smoothing intervals. The important point to be seen from Table 4 is that for the same basic system parameters the navigation-system accuracies are significantly better for a lunar orbit than for an earth orbit. Such error reductions are to be expected, because both the radius and mass of the moon are less than those of the earth.

Exact Smoothing

Data Processing

The principal difficulty with the polynomial filtering approach just discussed is the truncation error arising from approximation of the measured quantities by polynomials. This difficulty can be avoided by using the fact that the motion of the vehicle can be completely specified by four constants, since it is governed by a fourth-order system of differential equations, assuming the plane of motion to be known. For the problem of motion in the field of an oblate planet, the differential equations cannot be solved in closed form, but can be integrated numerically. The problem then reduces to finding those initial conditions that best fit the measured data. This problem may be solved by assuming an approximate set of initial conditions and linearizing about them. Then the best linearized estimate of the change in initial conditions required to fit the data is obtained from a linear filter. This is used to correct the assumed initial conditions and the process is repeated. This approach was used by Satyendra and Bradford.[10] However, their system did not use planet disk width data. It will be shown that the use of disk width data improves system navigational accuracy appreciably.

The process is essentially similar, but much simpler to mechanize, in the case of motion about a spherical planet. In this case, the motion may be described as follows:

$$E - \epsilon \sin E = \omega(t - T_p) \tag{10}$$

$$r = a(1 - \epsilon \cos E) \tag{11}$$

$$\theta = \theta_0 + 2 \tan^{-1}\left[\left(\frac{1+\epsilon}{1-\epsilon}\right)^{1/2} \tan\frac{E}{2}\right] \tag{12}$$

$$a = (g^{1/2}R/\omega)^{2/3} \tag{13}$$

The position of the vehicle (r, θ) at any time t is then specified by the four constants θ_0, ϵ, T_p, and ω. The measurements actually made are θ, the direction of the local vertical, and ϕ, half the disk width. These are also determined by the four constants given, since

$$\phi = \sin^{-1}(R/r) \tag{14}$$

The measurements and the desired four constants are not linearly related however. Hence, again an iterative procedure must be employed. An approximate set of constants $\theta_0°$, $\epsilon°$, $T_p°$, and $\omega°$ is chosen. From these, estimates $\theta°$ and $\phi°$ of what the measurements should be are derived by Eqs. (10–14). Linearizing Eqs. (10–14), and neglecting higher-order terms, one obtains

$$V_K = B_K \gamma \tag{15}$$

where

$$V_K = \begin{bmatrix} \theta_M - \theta° \\ \phi_M - \phi° \end{bmatrix}_{t=t_K}$$

$$\gamma = \begin{bmatrix} \theta_0 - \theta_0° \\ \epsilon - \epsilon° \\ T_p - T_p° \\ \omega - \omega° \end{bmatrix} \tag{16}$$

$$B_K = \begin{bmatrix} \frac{\partial\theta°}{\partial\theta_0°} & \frac{\partial\theta°}{\partial\epsilon°} & \frac{\partial\theta°}{\partial T_p°} & \frac{\partial\theta°}{\partial\omega°} \\ \frac{\partial\phi°}{\partial\theta_0°} & \frac{\partial\phi°}{\partial\epsilon°} & \frac{\partial\phi°}{\partial T_p°} & \frac{\partial\phi°}{\partial\omega°} \end{bmatrix}_{t=t_K}$$

at each measurement point t_K.

For n sets of measurements there are n sets of Eq. (15). Since the measurements are corrupted by noise, the Eq. (15) cannot in general all be satisfied exactly by any choice of constants γ. The error is given by

$$\delta_K = B_K\gamma - V_K \tag{17}$$

The best least squares estimate for equally weighted measurements is defined as that minimizing δ^2, where

$$\delta^2 = \sum_{K=1}^{n} \delta_K{}^T \delta_K \tag{18}$$

Substituting (17) into (18)

$$\delta^2 = \sum_{K=1}^{n} (\gamma^T B_K{}^T - V_K{}^T)(B_K\gamma - V_K) \tag{19}$$

To minimize δ^2 it is necessary that $\Delta\delta^2 = 0$ for an arbitrary

Table 4 Comparison of navigation system performance for earth and lunar orbits

Minimum root-sum-squares, error in	Earth orbit; R_E = 3440 naut miles, a = 3640 naut miles	Lunar orbit; R_E = 937 naut miles, a = 1037 naut miles
X, ft	5240	1300
X, fps	45.4	8.33
r, ft	1480	630
$\dot{r}$, fps	14.9	5.24

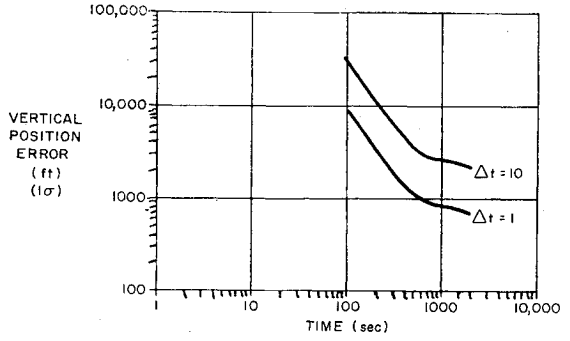

Fig. 3 Vertical position error vs smoothing time.

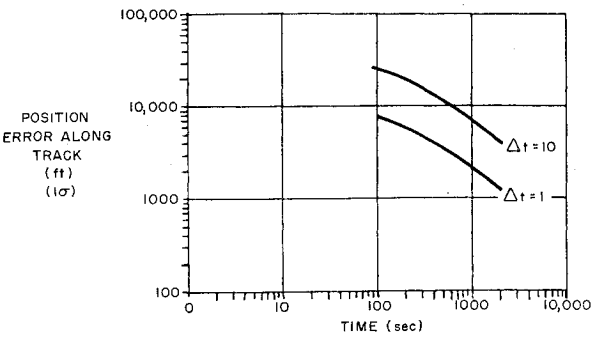

Fig. 4 Position error along track vs smoothing time.

change $\Delta\gamma$ in the constants γ. Hence,

$$\Delta\delta^2 = 0 = 2\Delta\gamma^T \sum_{K=1}^{n} B_K{}^T(B_K\gamma - V_K) \tag{20}$$

Thus the best least squares estimate of γ must satisfy

$$\left(\sum_{K=1}^{n} B_K{}^T B_K\right)\gamma = \sum_{K=1}^{n} B_K{}^T V_K \tag{21}$$

Defining

$$\sum_{K=1}^{n} B_K{}^T B_K = N \tag{22}$$

the solution to Eq. (21) may be written

$$\gamma = N^{-1} \sum_{K=1}^{n} B_K{}^T V_K \tag{23}$$

Equation (23) gives the best estimate of the true constants θ_0, ϵ, T_p, and ω on a linearized basis. It should be noted that, even though n sets of measurements are taken, it is only necessary to invert a 4×4 matrix to determine γ. To account for nonlinearities, the values of these constants obtained from Eq. (23) are taken as new estimates $\theta_0°$, $\epsilon°$, $T_p°$, and $\omega°$, and the process is repeated. The iteration should be rapidly convergent, since it amounts to Newton's method when $n = 2$.

The principal disadvantage of this procedure appears to be the formidable amount of data reduction, requiring a digital computer. This data reduction may not be much greater than that required for polynomial smoothing, however, since relatively infrequent measurements may be taken over a much longer smoothing interval, as there is no truncation error. In any case, the generalized least squares approach will give greater accuracy for the same data and its use is imperative in the system applications where the utmost accuracy is necessary.

Error Analysis of the Exact Smoothing Technique

The next part of the problem is to analyze the errors resulting from this procedure. The covariance matrix of the errors in the orbital parameters is the most convenient form to use to express system errors. If $\tilde{\gamma}$ represents the error vector of the orbital parameters θ_0, ϵ, T_p, and ω, then the covariance matrix is defined as

$$\text{cov}(\tilde{\gamma},\tilde{\gamma}) = E(\tilde{\gamma},\tilde{\gamma}^T) \tag{24}$$

where $E(\ )$ denotes the expected value operator. The diagonal terms in the covariance matrix give the variances of the errors in the orbital elements, and the off-diagonal elements give the cross correlations between these errors.

If $\theta_0°$, $\epsilon°$, $T_p°$, and $\omega°$ are taken as the true values on the trajectory, γ vanishes, and consideration of Eq. (17) reveals that $V_K = \delta_K$, the measurement error. Substituting into Eq. (23) to obtain $\tilde{\gamma}$,

$$\tilde{\gamma} = -N^{-1} \sum_{K=1}^{n} B_K{}^T \delta_K \tag{25}$$

For independent and equally weighted measurements, the covariance matrix of the input errors δ_K is

$$E(\delta_K \delta_j{}^T) = \begin{cases} \sigma^2 I & K = j \\ 0 & K \neq j \end{cases} \tag{26}$$

where I is the unit matrix, and σ^2 is the variance of the measurement error. Substituting Eqs. (25) and (26) into Eq. (24),

$$E(\tilde{\gamma},\tilde{\gamma}^T) = \sigma^2 N^{-1}\left(\sum_{K=1}^{n} B_K{}^T B_K\right) N^{-1} \tag{27}$$

Application of the definition (22) of N then yields

$$E(\tilde{\gamma},\tilde{\gamma}^T) = \sigma^2 N^{-1} \tag{28}$$

This defines the error in the orbital constants, and it remains now to find the error in position and velocity at some desired time t_1 resulting from errors in these constants.

If the errors are small, linearization about the true values is valid. Thus, letting $\tilde{r}$, $\tilde{\dot{r}}$, $\tilde{\theta}$, and $\tilde{\dot{\theta}}$ be errors in position and velocity in polar coordinates,

$$\begin{bmatrix} \tilde{r} \\ \tilde{\dot{r}} \\ \tilde{\theta} \\ \tilde{\dot{\theta}} \end{bmatrix} = \begin{bmatrix} \frac{\partial r}{\partial\theta_0} & \frac{\partial_r}{\partial\epsilon} & \frac{\partial r}{\partial T_p} & \frac{\partial r}{\partial\omega} \\ \frac{\partial\dot{r}}{\partial\theta_0} & \frac{\partial\dot{r}}{\partial\epsilon} & \frac{\partial\dot{r}}{\partial T_p} & \frac{\partial\dot{r}}{\partial\omega} \\ \frac{\partial\theta}{\partial\theta_0} & \frac{\partial\theta}{\partial\epsilon} & \frac{\partial\theta}{\partial T_p} & \frac{\partial\theta}{\partial\omega} \\ \frac{\partial\dot{\theta}}{\partial\theta_0} & \frac{\partial\dot{\theta}}{\partial\epsilon} & \frac{\partial\dot{\theta}}{\partial T_p} & \frac{\partial\dot{\theta}}{\partial\omega} \end{bmatrix}_{t=t_1} \begin{bmatrix} \tilde{\theta}_0 \\ \tilde{\epsilon} \\ T_p \\ \tilde{\omega} \end{bmatrix} \tag{29}$$

The partial derivatives in this equation may be evaluated from Eqs. (10–13). Abbreviating Eq. (29) as

$$\tilde{Z} = A\tilde{\gamma} \tag{30}$$

the covariance matrix of Z is

$$E(\tilde{Z}\tilde{Z}^T) = AE(\tilde{\gamma}\tilde{\gamma}^T)A^T \tag{31}$$

Substituting for $E(\tilde{\gamma},\tilde{\gamma}^T)$ from Eq. (28),

$$\text{cov}(\tilde{Z},\tilde{Z}) = E(\tilde{Z}\tilde{Z}^T) = \sigma^2 A N^{-1} A^T \tag{32}$$

Again, the diagonal elements of $\text{cov}(\tilde{Z},\tilde{Z})$ are the variances of the position and velocity errors, and the off-diagonal elements represent cross correlation terms.

A digital computer program was written to evaluate Eq. (32). The nominal orbit and input errors used in this analysis

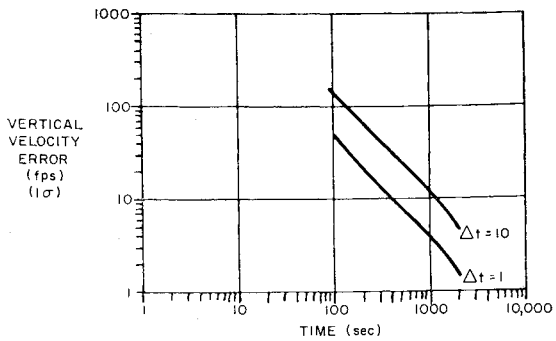

Fig. 5 Vertical velocity error vs smoothing time.

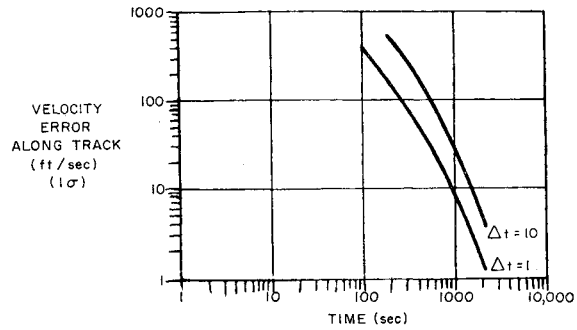

Fig. 6 Velocity error along track vs smoothing time.

are the same as those used in the polynomial smoothing analysis, which are listed previously (after Eq. 9). Typical plots of position and velocity errors as a function of smoothing time for two different data sampling rates are shown in Figs. 3–6. Because no truncation error exists, the error is seen to decrease steadily and quite rapidly as a function of smoothing time, and it is apparent that any desired error level can be achieved merely by smoothing over a long enough time interval. It should be noted that in an actual application such as a relatively low-altitude earth orbit, indefinitely long smoothing time using an elliptical model may not be attainable because of small perturbations that generate a nonelliptical orbit and act in exactly the same way as polynomial truncation terms in limiting the usable smoothing time. For the elliptical model and orbit studied here, smoothing times of about 1-orbit rotation appear reasonable. From the data shown in Figs. 4 and 6, it can be seen that such a smoothing time produces velocity errors of 0.1 to 1 fps, and position errors less than 1000 ft for earth orbits. In addition, Table 5 is presented to show the accuracy improvement if the exact smoothing navigation system is used in a lunar orbit. The smoothing time is about one-eighth to one-fourth of an orbit and is the same as that used in Table 4 for the polynomial system. Extending the exact system smoothing time results in velocity errors less than 0.1 fps and position errors less than 100 ft for a 2-mrad angular noise on the measurements.

Such accuracy is excellent for most system applications considered today and is quite suitable for both the earth orbital rendezvous mission and the lunar landing mission.

In order to compare navigation accuracies with and without disk width data, 1000 measurements were assumed to be taken over a complete orbital period for a 4255-naut mile earth satellite. In agreement with Ref. 10, angular root-mean-square measurement errors of 1 min of arc were used. The resultant errors in position and velocity are compared in Table 6.

It can be seen that considerable improvements occur in X, r, and $\dot{r}$, whereas no improvement occurs in $\dot{X}$. No improvement should be expected in $\dot{X}$ because disk width measurements on a spherical planet supply essentially no information about transverse velocity. However, the improvements that do occur, especially that in $\dot{r}$, are significantly better than the factor of $2^{1/2}$ to be expected simply from taking twice as many measurements. The large improvement occurs primarily because radial velocity can be related directly to disk width rate of change.

Table 5 Exact smoothing navigation system performance for earth and lunar orbits

Error in	Earth orbit; R = 3440 naut miles, a = 3640 naut miles	Lunar orbit; R = 937 naut miles, a = 1037 naut miles
X, ft	1810	544
$\dot{X}$, fps	5.5	1.6
r, ft	855	325
$\dot{r}$, fps	4.5	1.2

Table 6 Improvement obtained by including disk width data

Error in	Local vertical only[10]	Local vertical plus disk width
X, ft	840	570
r, ft	420	240
$\dot{X}$, fps	0.32	0.32
$\dot{r}$, fps	0.71	0.11

Conclusions

Two self-contained navigation systems have been described for use in a satellite vehicle travelling around the earth or the moon in an elliptical orbit. The performance of the poly-

Table 7 Comparative errors for polynomial approximation and exact least squares smoothing for a 200-naut mile orbit around the earth

ϵ	0.0275	0.00275	0.0275	0.0275	Eccentricity
Δt	1	1	10	1	Sample interval, sec
σ	2	2	2	5	Measurement error, mrad
T_r	900	1500	1100	1100	Radial smoothing time, sec
T_θ	1100	1900	1500	1400	Angular smoothing time, sec
σ_r polynomial exact	1400	1150	4120	3320	Vertical position
	855	935	2580	2060	error, ft
$a\sigma_\theta$ polynomial exact	5240	4060	14600	11800	Position error along
	1810	1390	4830	4020	track, ft
$\sigma_{\dot{r}}$ polynomial exact	14.9	6.92	32.2	28.6	Vertical velocity
	4.46	2.48	10·9	8.67	error, fps
$a\sigma_{\dot{\theta}}$ polynomial exact	45.4	21.1	98.1	86.1	Velocity error along
	5.51	1.62	9.65	9.17	track, fps

nomial smoothing system is shown to be adequate in altitude determination accuracy, but marginal in velocity accuracy, for an earth orbital rendezvous mission. On the other hand, this system may be adequate for a lunar landing mission depending upon the characteristics of the lunar parking orbit. The performance of the exact smoothing scheme is shown to be more than adequate for both of these missions. However, the exact smoothing system is more complicated than the polynomial system. Whether or not this complication is justified by the improved results depends upon mission requirements of the vehicle.

Comparative position and velocity errors for the exact least squares fit and a third-order polynomial approximation are presented in Table 7. The smoothing times were chosen to be the optimal smoothing times for the polynomial, considering the data accuracy and rate, and the truncation errors to be expected. It is seen that the exact fit gives uniformly smaller errors and that the improvement in position error may be a factor of two or more, whereas that in velocity may be an order of magnitude. For shorter somoothing times the errors would be more nearly comparable. On the other hand, for longer smoothing times the errors for the polynomial approximation would increase, whereas those for the exact fit would continue to decrease rapidly. It is particularly instructive to compare the first and third columns in Table 7. Here the only difference is the data rate, one sample per second in the first case and one sample every 10 sec in the second. It is seen that the error from the exact fit at the low data rate is generally less than the error from the polynomial approximation at the higher data rate. Hence, the apparent complexity of the exact fit is not a measure of the total number of arithmetic operations to be performed. This may actually be reduced for the same accuracy. Nevertheless, exact fitting requires a digital computer whereas polynomial smoothing only requires a relatively simple digital differential analyzer. If a digital computer must be carried for other parts of the overall mission, its capacities may be put to good use in performing a least squares fit using the exact model. Thus, if the satellite navigation system uses an inherently exact smoothing scheme, instrumentation requirements may be relaxed.

References

[1] "Rendezvous guidance and mechanization for orbital launch operations," Raytheon Co. Rept. BR-1469B (December 20, 1961); unclassified.

[2] Duke, W., "Lunar landing problems," Lunar Flight Symposium, Am. Astronaut. Soc. Denver, Colo. (December 29, 1961).

[3] Lunde, B., "Horizon sensing for attitude determination," Goddard Memorial Symposium, Am. Astronaut. Soc. Preprint 62–47 (March 1962).

[4] Worsmer, E. and Arck, M., "Infrared navigation sensors for space vehicles," ARS Preprint 1928–61 (1961).

[5] Kendall, P. and Stalcup, R., "Attitude reference devices for space vehicles," Proc. Inst. Radio Engrs. **48**, 765–770 (April 1960).

[6] "All altitude horizon sensors," Barnes Engineering Co. Special Sheet 13-160 (April 15, 1961).

[7] Kovit, B., "IR horizon sensor guides planetary orbiting," Space/Aeronaut. **35**, 131–133 (February 1961).

[8] "Lunar landing," Raytheon Co. Rept. BR-1394 (October 20, 1961); unclassified.

[9] Nesline, F. W., Jr., "Polynomial filtering of signals," Inst. Radio Engrs. Trans. Military Elecron. pp. 531–542 (June 1961).

[10] Satyendra, K. N. and Bradford, R. E., "Self-contained navigational system for determination of orbital elements of a satellite," ARS J. **31**, 949–956 (1961).

OCTOBER 1963 AIAA JOURNAL VOL. 1, NO. 10

Buckling of a Truncated Hemisphere under Axial Tension

JOHN C. YAO*

Northrop Norair, Hawthorne, Calif.

This report is concerned with the theoretical evaluation of the buckling strength of a truncated hemisphere under axial tensile load. The edges of the shell are assumed to be restrained from moving radially or from rotating. Theoretical results were obtained by Vlasov's small deflection theory and Galerkin's method. The quick convergence of the series solution is demonstrated. Comparison of theoretical values with a few available experimental results is given.

Nomenclature

A_n, B_n = coefficients of series expansion for radial deflection and stress function, respectively
a = mean radius (see Fig. 2)
E = Young's modulus
l = $\sin\alpha$
m = number of buckle waves in the circumferential direction
P = axial tensile load per unit circumferential length at the shell equator
q = radial load per unit middle surface area
$T_\phi, T_\theta, T_{\phi\theta}, T_{\phi\theta}$ = additional force components in the buckled shell
$T_{\phi 0}, T_{\theta 0}$ = membrane force components prior to buckling
t = shell thickness
w = radial buckling displacement of a middle surface point
x = $\sin\phi$
α = altitude angle of the truncated edge (see Fig. 2)
θ, ϕ = spherical coordinates (see Fig. 2)
μ = Poisson's ratio
Φ = stress function
∇^2 = Laplace's operator $[(\partial^2/a^2\partial\phi^2) - \tan\phi(\partial/a^2\partial\phi) + \sec^2\phi(\partial^2/a^2\partial\theta^2)]$

Received January 25, 1963; revision received June 21, 1963. The author wishes to take this opportunity to thank A. J. Carah, Chief Engineer, Missile Systems, Douglas Aircraft Company Inc., for permission to publish the testing results; he also wishes to thank his supervisor, P. Seide, for invaluable comments and suggestions. The assistance of J. Yamane in checking the algebra and of J. Riley and G. Johnson for programming support also is acknowledged.

* Senior Scientist.